ABOUT TWO-TIME MODEL AND THE SPATIAL DISTRIBUTION OF BEC MAGNONS

A Thesis

by

HAICHEN JIA

Submitted to the Graduate and Professional School of
Texas A&M University
in partial fulfillment of the requirements for the degree of

MASTER OF SCIENCE

Chair of Committee,	Valery L. Pokrovsky
Committee Members,	Wayne Saslow
	Alexander Finkel'stein
	Donald Naugle
	Gregory Berkolaiko
Head of Department,	Grigory Rogachev

December 2021

Major Subject: Physics

Copyright 2021 Haichen Jia

ABSTRACT

Since the Bose-Einstein condensation (BEC) of magnons in ferromagnetic films was realized, it has drawn much attention due to the unique property of magnon spectrum. Namely, the BEC has two components corresponding to the two ground states of magnons. In recent years, experiments showed the repulsive nature of magnons and the spatial separation of condensate magnon cloud, contradicting the existing quasi-equilibrium theory. To explain such phenomena, we found the error in this theory: The equilibrium state of the two components is never reached, and, on the contrary, the flipping rate of magnon from one component into the other is much lower than its self-decay rate.

In the following part, we proposed the two-time model, treating magnons as classical particles. The model is based on the continuity equation of magnon creation, annihilation, and flow. With its help, we can not only explain the experimental findings, but also explore a fundamental question: the spatial distribution of BEC magnons.

DEDICATION

To my parents and my advisor. Moreover, to my girlfriend, Qiuyue, who stood beside me on the hardest days.

ACKNOWLEDGMENTS

I want to thank my advisor Professor Pokrovsky, my advisor, for all the help and guidance he provided. Professor Pokrovsky is very kind and patient to students, while his deep thinking in physics impressed me greatly. His curiosity and enthusiasm towards physics have encouraged me to go much farther than I thought.

Also, I want to thank Dr. Gang Li, who answered so many of my weird questions and discussed the details in calculations with me. His experience in this field saved me much time.

I also want to thank Professor Saslow for his kind advice on the wording of this work and how to make a presentation more understandable.

And I thank all my friends, especially Mr. Haoyu Zhang, Mr. Zifeng Luo, Mr. Tianyang Ma, and Mr. Zhenming Fang, for the good talks we had during the pandemic.

Lastly, thank my girlfriend Qiuyue, I couldn't have gone this far without you.

CONTRIBUTORS AND FUNDING SOURCES

Contributors

This work was supervised by a dissertation committee consisting of Professor Valery L. Pokrovsky (advisor) and Professor Wayne Saslow, Alexander Finkel'stein, and Donald Naugle of the Department of Physics and Astronomy, and Professor Gregory Berkolaiko of the Department of Mathematics.

All work conducted for the thesis (or) dissertation was completed by the student, with the guidance of Professor Valery L. Pokrovsky and the advice from Dr. Gang in our group.

Funding Sources

Graduate study was financially supported by my advisor Dr. Valery Pokrovsky under the auspices of account 512982 of the William Thurman'58 Chair in Physics, and also the teaching assistantship from the department of Physics and Astronomy at Texas A&M University.

NOMENCLATURE

OGAPS	Office of Graduate and Professional Studies at Texas A&M University
BEC	Bose-Einstein condensation
YIG	Yttuium iron garnet
BLS	Brillouin light scattering
BECM	Bose-Einstein condensate of magnons
L	length of the sample along $\hat{z}$ direction
l	width of the control line
ℓ	dipolar length
d	sample thickness
$\mathbf{H}$	the strong uniform external magnetic field
$\mathbf{h}(z)$	the extra non-uniform magnetic field as a potential well
$\mathbf{Q}$	the in-plane wave vector of condensate magnons (positive branch)
n_0	equilibrium density of BEC magnons without the presence of $\mathbf{h}(z)$
$n(z,t)$	density of BEC magnons with $\mathbf{h}(z)$ applied
$\tau_{min-min}$	inter-minima relaxation time
τ_m	lifetime of condensate magnons
$j(z)$	current density of magnon flow

TABLE OF CONTENTS

Page

LIST OF FIGURES

FIGURE Page

1. INTRODUCTION

Bose-Einstein condensation (BEC) of magnons was first discovered in 2006 by the Münster University experimental team led by S.O. Demokritov [1]. The experiment was performed with an Yttrium Iron Garnet (YIG) film, or $\mathrm{Y_3Fe_2(FeO_4)_3}$ under steady state pumping at room temperature. The Brillouin light scattering (BLS) was used to detect magnon density. BEC of magnon occurs when chemical potential reaches the minimal energy of magnons.

Bose-Einstein condensate of magnons (BECM) received much attention in the following years, because of its unique properties. The spectrum of magnons in the film is quite non-trivial. Let's set the external magnetic field $\mathbf{H}$ directs towards $\hat{z}$, parallel to the film, while $\hat{x}$ is perpendicular to film. The spectrum has two symmetric minima: $\omega_{\min} \approx \frac{eH}{m^*c}$, $\pm\mathbf{Q} = (0, 0, \pm Q)$ ($Q = \frac{\left(2\pi^3\right)^{1/4}}{\sqrt{\ell d}}$ [2]), and a local maximum at $\mathbf{k} = (0, 0, 0)$. $\omega_{\max} \approx \frac{e}{m^*c}\sqrt{H\left(H + 4\pi M\right)}$ corresponds to the ferromagnetic resonance.

The presence of two ground states with equal energy makes BECM different from the usual BEC system. Naturally, one would wonder: will the BEC of magnons have two components? And how do the two components interact? In 2012, the same group [3], observed the interference pattern of two condensate components. Although the two ground states share the same energy, their density may vary significantly, and the interference found to be weak, with the depth of interference pattern only about 3-4% of total density.

In 2013, Li, Saslow, and Pokrovsky [4] proposed the quasi-equilibrium theory, which explained the asymmetry of the density of two components. Considering magnon interaction, (especially magnon-non-conserving terms in 4th order Hamiltonian), the distribution was calculated by minimizing total energy. The prediction was: for the film thickness $d < d_c \sim 100$nm, the system stays in a high-contrast symmetric state, while for $d > d_c$ it is in a low-contrast non-symmetric state. For small thickness $d < 40$nm, there remains only one minimum at zero wave vector.

However, two recent reports of the Demokritov team [5] [6] displayed several important facts contradicting existing theories of the BECM. Although a complete theoretical description of these

experiments is still in development, we will present simplified theoretical arguments to determine the properties of the uniform stationary BECM established under the steady state parametric pumping that follows from the experimental facts.

2. LITERATURE REVIEW

2.1 Experiment I

In the first experiment [5], the sample of YIG film was a square with the side $L = 4$mm, and thickness $d = 5\mu$m, which mounts on the interface of the dielectric resonator. The constant magnetic field $H = 600$Oe along $\hat{z}$ fixed the spontaneous magnetization M in the same direction. The experiment was performed at room temperature that is below the ferromagnetic phase transition. The value of spontaneous magnetization at this temperature is $M = 109.4G$. A nanometer-thick golden stripe of width $l = 10\mu$m was inserted between the sample and resonator, along direction $\hat{y}$ (perpendicular to $\mathbf{H}$ but within the plane of film), so that the central line of the stripe divided the sample into two equal halves. Let the upper surface of the sample be the plane $x = 0$. The length of the stripe was a few centimeters. It is much larger than all other linear sizes of the system and in all calculations will be treated as infinity. During the experiment, the steady current I through the stripe created magnetic field $\mathbf{h}$, whose z-component h_z could be either antiparallel or parallel to the field H, representing a potential well or potential barrier for magnons, respectively. The absolute value of h_z varied in limits between 10 to 20 Oe. In all measurements, the strong inequality $|h_z| \ll H$ was satisfied. A schematic drawing of the experimental device is shown in Fig. 2.1 (a). (Adapted from "Schematic of the experiment." in [5])

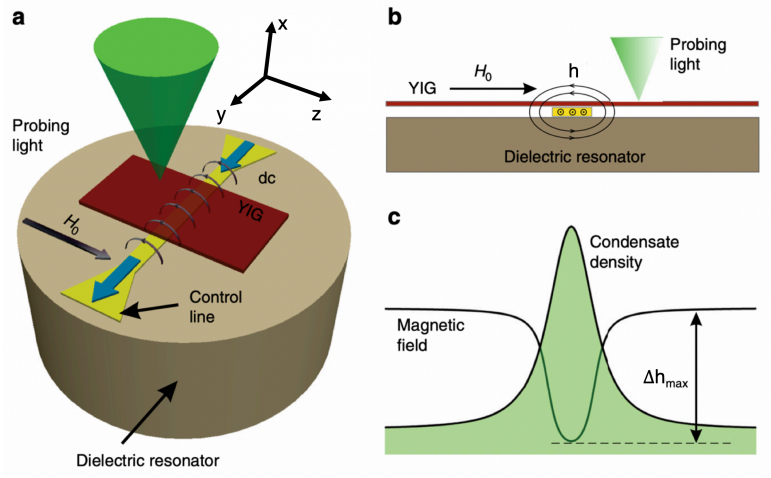

Figure 2.1: Experimental setup. a) A general view. The sample YIG film is placed on the Dielectric resonator, which pumps magnon constantly into the film. The static uniform outside magnetic field is $\mathbf{H}_0$. The yellow stripe is the control line, which creates an extra magnetic field $\mathbf{h}$ as a potential well for magnons. The green cone stands for the laser probe used in the BLS method to detect the density of BEC magnons. b) A cross-section of the system. c) A schematic plot of condensate magnon density and magnetic field versus z coordinate. Adapted from "Schematic of the experiment." in [5]. Used under https://creativecommons.org/licenses/by/4.0/.

There are several length scales in the problem. One of them is the dipolar length ℓ that defines a scale at which the exchange and dipolar interactions are of the same order of magnitude. It is defined by the exchange interaction term in the Landau-Lifshitz Hamiltonian written in the form:

$$H_{ex} = \frac{D}{2} \int (\nabla \mathbf{M})^2 \, d^3x, \tag{2.1}$$

where $\mathbf{M}$ is the vector of magnetization and D stands for renormalized exchange constant. The dipolar length is defined as $\ell = \sqrt{D}$. For YIG at room temperature, $\ell = 38nm$ [7]. The same length ℓ is also called in literature the exchange length. The second characteristic length l is the width of the gold plate generating inhomogeneous magnetic field in experiment I. The third length is the distance between the golden plate and the sample x_0. Two other lengths are the sample size: its thickness d and the length of the side of the square sample $L = 4mm$. In the experimental device, strong inequalities $\ell \ll x_0 \ll d < l \ll L$ were satisfied.

The main result obtained in experiment I is the direct evidence that the magnons of condensate repel each other. To show that, the experimenters switched off the pumping and followed how the shape of the peak of condensate density changes with time. The results are shown in Fig. 2.2 (a), where the relative density $n\left(z,t\right)/n\left(0,t\right)$ is displayed for several consecutive moments after switching off the pumping $t=0$. Fig. 2.2 (b) shows the exponential decay with different decay time for different points of the initial density profile. Combining the two parts of Fig. 2.2, we can see that: While the average condensate density exponentially decreases with time, the width of the profile decreases as well. In other words, the larger the average magnon density is, the broader its distribution grows in space. This is direct evidence of their repulsion.

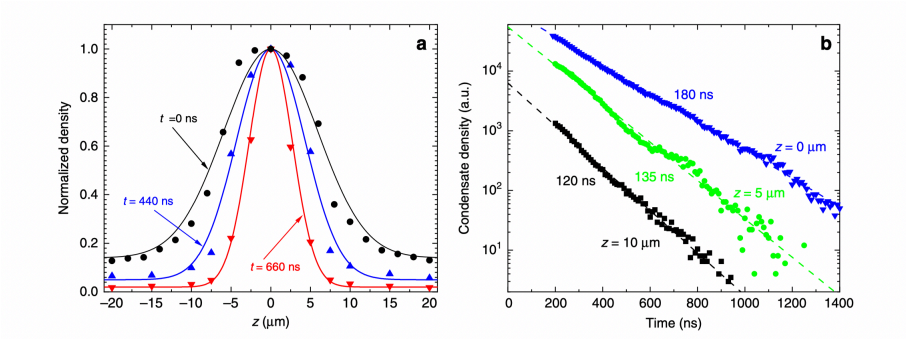

Figure 2.2: Decaying of magnon density after pumping is turned off. a) Normalized spatial density of condensate magnons, recorded at different delay time, in a potential well with $\Delta H_{max}=-10$Oe. Solid lines are a guide for the eye. b) Time dependence of condensate density at different positions. Dashed lines are exponential fit of data. Effective decay times are labeled using the same color as the corresponding data. Reprinted from "Time evolution of the condensate density in a potential well after turning the microwave pumping off." in [5]. Used under https://creativecommons.org/licenses/by/4.0/.

2.2 Experiment II

The second experiment [6] was performed in the same geometry as the first one. A short pulse of magnetic field submitted to magnons of condensate an additional amount of energy $\Delta\varepsilon$. It splits the condensate initially distributed between two minima into four moving condensate clouds corresponding to four points of the magnon spectrum with energy $\varepsilon_{\min}+\Delta\varepsilon$ $(0<\Delta\varepsilon<\varepsilon_{\max}-\varepsilon_{\min})$.

These beams have finite velocities. Listing in the order of increasing k_z, velocities of 4 clouds are $-v_1, v_2, -v_2, v_1$, which are equal to derivatives $\frac{d\varepsilon}{dk}$ in the four points of the spectrum. Such a motion of the beams was observed in experiment II as is shown in Fig. 2.3 (a) (Adapted from "Idea of the experiment." in [6]). The clouds eventually smear out since the field in the pulse is non-uniform, and $\Delta\varepsilon$ depends on z. The clouds display some asymmetry for reflection $k_z \Leftrightarrow -k_z$, but it is not strong.

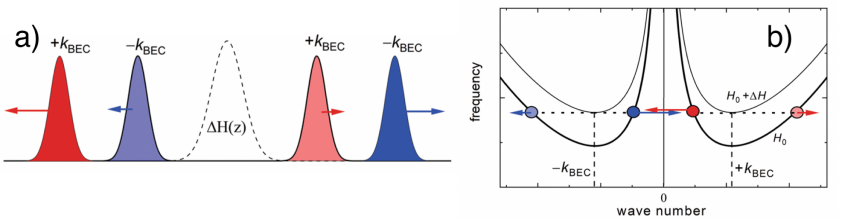

Figure 2.3: a) Schematic drawing of the splitting of the 4 clouds in real space. b) Magnon spectrum after the pulse is applied. The thick curve is the spectrum at the center, where magnetic field is $H_0+\Delta H$. And the thin curve is spectrum far away from the center. The arrows show schematically the velocities (in real space) of the corresponding cloud. Adapted from "Idea of the experiment." in [6]. Used under https://creativecommons.org/licenses/by/4.0/.

2.3 Quasiequilibrium theory

In the article [4], it was assumed that the weakly interacting gas of magnons relaxes to the equilibrium state with non-zero chemical potential μ. It happens if the relaxation time τ_{rel} is much less than the lifetime of magnons. In the basic approximation of non-interacting magnons, the energy does not depend on the distribution of magnons between two minima, as long as the total density of magnons $n = n_+ + n_-$ is fixed. This degenerecy is lifted by interaction. The general bilinear form of the interaction free energy per unit volume is:

$$F_{int} = \frac{A}{2}\left(n_+^2 + n_-^2\right) + Bn_+n_- + C\sqrt{n_+n_-}\,(n_+ + n_-)\cos\left(\phi_+ + \phi_-\right) + \frac{D}{2}\left(n_+^2 + n_-^2\right)\cos 2\left(\phi_+ + \phi_-\right) \tag{2.2}$$

The calculation of coefficients A and B by Tupitsyn et al. and by F. Li et al. showed $A < 0$, $B > 0$ and $|A| \ll B$ for a thick film $d \gg \ell$. The coefficients C and D found first in the work by F. Li et al. and recalculated in [8] have magnitudes much less than $|A|$. Nevertheless, the coefficient C and D are important. If they are equal to zero, one of the two condensate densities n_+ or n_- will be zero in the equilibrium state. The coefficient C makes both densities finite, although one of them is much less than another. It also results in the phase trapping: the phase $\phi = \phi_+ + \phi_-$ is equal to 0 or π depending on the sign of the coefficient C. A rather simple calculation of minimal free energy of condensate for a thick film, at a fixed value of the total density n, gives the two solutions for the ratios $\frac{n_\pm}{n}$. One of them is

$$\frac{n_+^{(1)}}{n} \approx 1 - \frac{C^2}{4B^2}; \; \frac{n_-^{(1)}}{n} = \frac{C^2}{4B^2} \tag{2.3}$$

The second solution differs from the first by permutation of n_+ and n_-. These solutions are clearly strongly asymmetric. Thus, in a thick film of YIG, the interaction leads to a spontaneous violation of symmetry between the two condensates: the density of one of them becomes much larger than the other. Their free energy is equal to $F_{int} \approx \frac{An^2}{2} < 0$. [9] [10]. The attraction makes the homogeneous equilibrium state unstable. The free energy is minimized by a state with periodically repeated phase solitons. For different systems, such a state was first predicted by Sonin [2]. This conclusion contradicts experiment I by Borisenko et al. that has proved the repulsion of magnons.

2.4 Analysis

What went wrong in the quasi-equilibrium theory? The only possible conclusion is that complete equilibrium was not established in the magnon system. The most probable reason is that the inter-minima relaxation time $\tau_{min-min}$ is much longer than the lifetime of condensate magnons τ_m. Here we argue that it is indeed the case. The processes that flip the magnon from one minimum to the other and lead to the inter-minima equilibrium are i) Compton scattering of the low-energy magnon by a thermal magnon and ii) the direct 4th order processes of a coherent flip of condensate magnon interacting with a thermal magnon. Both these processes have very small probability

being proportional to the fourth power of a small non-linearity.

What is the uniform stationary state of the condensate? Since the magnons repel each other, the uniform stationary state of the condensate does not collapse. If the inter-condensate relaxation processes considered in the previous paragraph are negligible, then the stationary state of the condensate must be symmetric. The reason is that the interactions responsible for parametric pumping and for the finite magnon lifetime are identical for the two condensates. The weak inter-condensate relaxation processes lead to a weak spontaneous violation of the reflection symmetry. This prediction agrees with the inter-condensate interference structure of the condensate discovered by Novik-Boltyk et al. [11] In real experiments, it is difficult to avoid a weak asymmetry of the device that favors one of two slightly asymmetric stationary states. Such a device asymmetry can explain the asymmetry observed in experiment II by Borisenko et al. If the asymmetry is relatively small, then in eq. (2.2) the term Bn_+n_- is dominant and positive. This theoretical conclusion agrees with experiment I and makes the concept of weak spontaneous violation of the reflection symmetry self-consistent.

3. CALCULATION OF INTER-MINIMA RELAXATION TIME

Before proceeding to the theory, it is important to check that the inter-minima relaxation time is indeed much longer than the condensate lifetime. Below we briefly describe the amplitude representation method that we applied.

3.1 Hamiltonian

There are three terms in our Hamiltonian: exchange, Zeeman, and dipolar terms, denoted as H_{ex}, H_Z, and H_d, respectively:

$$\begin{aligned} H &= H_{ex} + H_z + H_d \\ H_{ex} &= -J \sum_{\langle i,j \rangle} \mathbf{S}_i \cdot \mathbf{S}_j \\ H_Z &= -g\mu_B \sum_i \mathbf{H} \cdot \mathbf{S}_i \\ H_d &= -\frac{1}{2}(g\mu_B)^2 \sum_{i \neq j} \frac{3(\mathbf{S}_i \cdot \hat{\mathbf{r}}_{ij})(\mathbf{S}_j \cdot \hat{\mathbf{r}}_{ij}) - \mathbf{S}_i \cdot \mathbf{S}_j}{r_{ij}^3} \end{aligned} \tag{3.1}$$

Here, $g \approx 2$ and μ_B are g-factor and Bohr magneton, respectively, and $\mathbf{H}$ is the external magnetic field. For exchange term, J is exchange integral, which is positive in ferromagnet material, and $\langle i, j \rangle$ means summing over nearest neighbor.

If we focus on long-wave magnons, meaning those with wavelength much larger than the lattice constant, we could rewrite the Hamiltonian using continuous field $\mathbf{S}(\mathbf{r}_i) = \mathbf{S}_i/a^3 = \mathbf{M}(\mathbf{r}_i)/(g\mu_B)$:

$$\begin{aligned} H_{ex} &= \frac{D}{2} \int (\nabla \mathbf{M})^2 \, d^3x \\ H_Z &= -\int \mathbf{H} \cdot \mathbf{M} d^3\mathbf{r} \\ H_d &= \frac{1}{2} \iint (\mathbf{M} \cdot \nabla)(\mathbf{M}' \cdot \nabla') \frac{1}{|\mathbf{r} - \mathbf{r}'|} d^3\mathbf{r} d^3\mathbf{r}' \end{aligned} \tag{3.2}$$

where D is already introduced as square of dipolar length. $\mathbf{M}' \equiv \mathbf{M}(\mathbf{r}')$, and $\nabla' \equiv (\partial_{x'}, \partial_{y'}, \partial_{z'})$.

3.2 Amplitude representation

The standard Holstein-Primakoff transformation turns the spin operator $\mathbf{S}$ into creation and annihilation operators:

$$\begin{aligned} S_j^+ &= \sqrt{2S}\left(1-\frac{a_j^\dagger a_j}{2S}\right)^{1/2} a_j \\ S_j^- &= \sqrt{2S}a_j^\dagger\left(1-\frac{a_j^\dagger a_j}{2S}\right)^{1/2} \\ S_j^z &= S - a_j^\dagger a_j \end{aligned} \tag{3.3}$$

where $S^\pm = S_x \pm iS_y$. When dealing with long wave magnons, one can rewrite this transformation in the classical limit, with amplitudes $\psi(\mathbf{r}_j)$, $\psi^*(\mathbf{r}_j)$ replacing a_j, a_j^*, and $\gamma \approx 2\mu_B$.

$$\begin{aligned} M_+(\mathbf{r}) &= \sqrt{\gamma}\psi(\mathbf{r})\sqrt{2M-\gamma\psi(\mathbf{r})\psi^*(\mathbf{r})} \\ M_-(\mathbf{r}) &= \sqrt{\gamma}\psi^*(\mathbf{r})\sqrt{2M-\gamma\psi(\mathbf{r})\psi^*(\mathbf{r})} \\ M_z(\mathbf{r}) &= M-\gamma\psi(\mathbf{r})\psi^*(\mathbf{r}) \end{aligned} \tag{3.4}$$

Here, the order of $\psi(\mathbf{r}_j)$, $\psi^*(\mathbf{r}_j)$ no longer matters, but they should obey the following Poisson bracket:

$$\{\psi(\mathbf{r}), \psi^*(\mathbf{r}')\} = -\frac{i}{\hbar}\delta(\mathbf{r}-\mathbf{r}') \tag{3.5}$$

In amplitude representation, the Hamiltonian is:

$$\begin{aligned} H_{ex} &= \frac{\gamma^2 D}{2}\int\left(\nabla\left(|\psi|^2\right)\right)^2 dV + \frac{\gamma D}{2}\int\left|\nabla\left(\psi\sqrt{2M-\gamma|\psi(\mathbf{r})|^2}\right)\right|^2 dV \\ H_z &= \gamma\mathcal{H}\int|\psi(\mathbf{r})|^2 dV \\ H_d &= \frac{1}{2}\iint\hat{\Omega}(\mathbf{r})\hat{\Omega}(\mathbf{r}')\frac{dVdV'}{|\mathbf{r}-\mathbf{r}'|} \end{aligned} \tag{3.6}$$

while

$$\hat{\Omega}(\mathbf{r}) = \left(M-\gamma|\psi|^2\right)\partial_z + \frac{\sqrt{\gamma\left(2M-\gamma|\psi|^2\right)}}{2}\left(\psi\partial_- + \psi^*\partial_+\right) \tag{3.7}$$

The current goal is to express the Hamiltonian with $\eta_{\mathbf{q}n}$ and $\eta^*_{\mathbf{q}n}$, which annihilates/creates a magnon with in-plane wave vector $\mathbf{q}$, and a quantum number n describes the modes in the $\hat{x}$ direction. What's more, the state corresponding to $\eta_{\mathbf{q}n}$ and $\eta^*_{\mathbf{q}n}$ should also be eigenstates of quadratic Hamiltonian H_2:

$$\begin{aligned}
H_2 &= H_{ex2} + H_{z2} + H_{d2} \\
H_{ex2} &= \gamma M D \int |\nabla\psi|^2 dV \\
H_{z2} &= \gamma\mathcal{H} \int |\psi|^2 dV \\
H_{d2} &= \frac{\gamma M}{4} \iint \frac{\left(\psi\partial_- + \psi^*\partial_+\right)\left(\psi'\partial'_- + \psi'^*\partial'_+\right)}{|\mathbf{r}-\mathbf{r}'|} dV dV'
\end{aligned} \tag{3.8}$$

Here $\mathcal{H}$ stands for external magnetic field. To perform the diagonalization, one should do an in-plane Fourier transform:

$$\begin{aligned}
\psi(\mathbf{r}) &= \sum_{\mathbf{q}} \chi_{\mathbf{q}}(x) \frac{e^{i\mathbf{q}\mathbf{r}}}{\sqrt{A}} \\
\chi_{\mathbf{q}}(x) &= \frac{1}{\sqrt{A}} \iint_{-\infty}^{\infty} \psi(\mathbf{r}) e^{-i\mathbf{q}\mathbf{r}} dy dz
\end{aligned} \tag{3.9}$$

where Poisson bracket of $\chi_{\mathbf{q}}(x)$ is: $\left\{\chi_{\mathbf{q}}(x), \chi^*_{\mathbf{q}'}(x')\right\} = -\frac{i}{\hbar}\delta_{\mathbf{q}\mathbf{q}'}\delta(x-x')$. After that we perform a Bogoliubov transform (done first by Holstein and Primakoff in [12]):

$$\begin{aligned}
\eta_{\mathbf{q}n} &= \int_{-d/2}^{d/2} \left[u_{\mathbf{q}n}(x)\chi_{\mathbf{q}}(x) + v_{\mathbf{q}n}(x)\chi^*_{-\mathbf{q}}(x)\right] dx \\
\chi_{\mathbf{q}}(x) &= \sum_n \left(u^*_{\mathbf{q}n}(x)\eta_{\mathbf{q}n} - v_{-\mathbf{q}n}(x)\eta^*_{-\mathbf{q}n}\right)
\end{aligned} \tag{3.10}$$

Here, $\eta_{\mathbf{q}n}$ ($\eta^*_{\mathbf{q}n}$) is the annihilation (creation) operator of magnon $(\mathbf{q}, n)$, where $\mathbf{q}$ is its in-plane wave vector, and n is the quantum number describing its mode in $\hat{x}$ direction. The Poisson bracket of $\eta_{\mathbf{q}n}$ is: $\left\{\eta_{\mathbf{q}n}, \eta^*_{\mathbf{q}'n'}\right\} = -\frac{i}{\hbar}\delta_{\mathbf{q}\mathbf{q}'}\delta_{nn'}$.

We required that $\eta_{\mathbf{q}n}$ and $\eta^*_{\mathbf{q}n}$ can diagonalize H_2. This is equivalent to:

$$\{H_2, \eta_{\mathbf{q}n}\} = i\omega_{\mathbf{q}n}\eta_{\mathbf{q}n} \tag{3.11}$$

where $\hbar\omega_{\mathbf{q}n}$ will be the energy of the corresponding state. Equation (3.11) can be used to solve for $u_{\mathbf{q}n}(x)$ and $v_{\mathbf{q}n}(x)$.

3.3 How to calculate inter-minima relaxation time

To calculate inter-minima relaxation time, first we need to isolate the relevant terms in the Hamiltonian. Two processes primarily concern us:

4-magnon process: A condensate magnon $(\mathbf{Q}, 0)$ reacts with a thermal magnon in state $(\mathbf{k}, n)$:

$$(\mathbf{Q}, 0) + (\mathbf{k}, n) \to (-\mathbf{Q}, 0) + (\mathbf{k} + 2\mathbf{Q}, n') \tag{3.12}$$

Compton process: A combination of two 3-magnon process:

$$(\mathbf{Q}, 0) + (\mathbf{k}, n) \to (\mathbf{k} + \mathbf{Q}, n'') \to (\mathbf{Q}, 0) + (\mathbf{k} + 2\mathbf{Q}, n') \tag{3.13}$$

The Feynman diagrams for these processes are shown in Fig. 4.

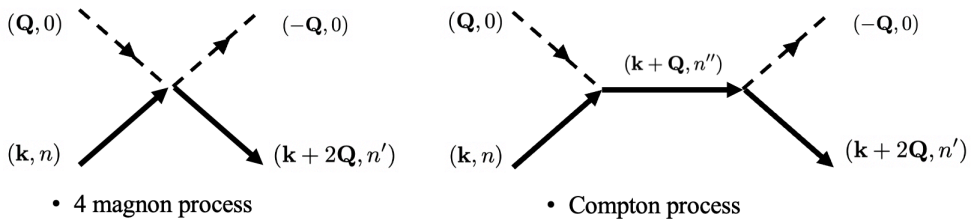

Figure 3.1: Feynman diagrams for two inter-minima flipping processes. Dashed lines stand for condensate magnons, while solid lines stand for thermal magnons.

Consider 4-magnon process first. The corresponding 4th order Hamiltonian (before Bogoli-

ubov transformation) reads:

$$H_{ex4} = \frac{\gamma^2 D}{4A} \int \sum_{\mathbf{q}_1,\mathbf{q}_2,\mathbf{q}_3,\mathbf{q}_4} \left[\chi^*_{\mathbf{q}_2}\chi^*_{\mathbf{q}_4} d_x\chi_{\mathbf{q}_1} d_x\chi_{\mathbf{q}_3} + \chi_{\mathbf{q}_1}\chi_{\mathbf{q}_3} d_x\chi^*_{\mathbf{q}_2} d_x\chi^*_{\mathbf{q}_4} \right.$$
$$\left. + \left(\mathbf{q}_1^2 + \mathbf{q}_2^2\right)\chi_{\mathbf{q}_1}\chi^*_{\mathbf{q}_2}\chi_{\mathbf{q}_3}\chi^*_{\mathbf{q}_4} - 4\mathbf{q}_1\mathbf{q}_2\chi_{\mathbf{q}_1}\chi^*_{\mathbf{q}_2}\chi_{\mathbf{q}_3}\chi^*_{\mathbf{q}_4}\right] \delta_{\mathbf{q}_1-\mathbf{q}_2+\mathbf{q}_3-\mathbf{q}_4} dx \tag{3.14}$$

and

$$H_{d4} = \frac{2\pi\gamma^2}{A} \iint \sum_{\mathbf{q}_1,\mathbf{q}_2,\mathbf{q}_3,\mathbf{q}_4,\mathbf{q}} \left\{ q_z^2 \chi_{\mathbf{q}_1}\chi^*_{\mathbf{q}_2}\chi'_{\mathbf{q}_3}\chi'^*_{\mathbf{q}_4}\delta_{\mathbf{q}_1-\mathbf{q}_2+\mathbf{q}}\delta_{\mathbf{q}_3-\mathbf{q}_4-\mathbf{q}} \right.$$
$$- \frac{1}{4}\chi_{\mathbf{q}_1}\chi^*_{\mathbf{q}_2}\left[\chi_{\mathbf{q}_3}\left(d_x + q_y\right) + \chi^*_{-\mathbf{q}_3}\left(d_x - q_y\right)\right]\left[\chi'_{\mathbf{q}_4}\left(d_{x'} - q_y\right) + \chi'^*_{-\mathbf{q}_4}\left(d_{x'} + q_y\right)\right] \tag{3.15}$$
$$\left. \times\delta_{\mathbf{q}_1-\mathbf{q}_2+\mathbf{q}_3+\mathbf{q}}\delta_{\mathbf{q}_4-\mathbf{q}} \right\} G_q\left(x - x'\right) dx dx'$$

where $G_q(x) = e^{-q|x|}/2q$ is the Green function of 1d Helmholtz equation.

After Bogoliubov transformation, we need to isolate the amplitude of the term $\eta_{\mathbf{Q}1}\eta_{\mathbf{k}n}\eta^*_{-\mathbf{Q}1}\eta^*_{(\mathbf{k}+2\mathbf{Q})n'}$, let us denote it as $T(\mathbf{k}, n, n')$. According to Fermi's golden rule, the rate of condensate flip process is:

$$\frac{1}{\tau_{4th}} = \sum_{\mathbf{k},n,n'} \frac{2\pi}{\hbar} |T(\mathbf{k}, n, n')|^2 [(N_{\mathbf{k},n} + 1)(N_{\mathbf{Q},1} + 1)N_{-\mathbf{Q},1}N_{\mathbf{k}',n'}$$
$$- N_{\mathbf{k},n}N_{\mathbf{Q},1}(N_{-\mathbf{Q},1} + 1)(N_{\mathbf{k}',n'} + 1)]\delta_{\varepsilon_{\mathbf{k},n}+\varepsilon_{\mathbf{Q},1}-\varepsilon_{-\mathbf{Q},1}-\varepsilon_{\mathbf{k}',n'}} \tag{3.16}$$

The calculation of flipping process due to exchange term is shown below.

The 4th-order terms in the exchange interaction can be separated into two classes: containing the transverse derivatives $H^{(1)}_{ex4}$ and not containing them $H^{(2)}_{ex4}$, where:

$$H^{(1)}_{ex4} = \frac{\gamma^2 D}{4A} \sum_{\mathbf{k},n} \int_{-\frac{\mathrm{d}}{2}}^{\frac{\mathrm{d}}{2}} dx \left(\eta_{\mathbf{k},n}\eta_{\mathbf{Q}} d_x \eta^*_{\mathbf{k}+2\mathbf{Q},n'} d_x \eta^*_{-\mathbf{Q}} + c.c.\right) \tag{3.17}$$

$$H^{(2)}_{ex4} = \frac{\gamma^2 D}{4A} \sum_{\mathbf{k},n} \int_{-\frac{\mathrm{d}}{2}}^{\frac{\mathrm{d}}{2}} dx \left(\mathbf{k}^2 + \mathbf{Q}^2 - 4\mathbf{k}\mathbf{Q}\right)\left(\eta_{\mathbf{k},n}\eta_{\mathbf{Q}}\eta^*_{\mathbf{k}+2\mathbf{Q},n'}\eta^*_{-\mathbf{Q}} + c.c.\right) \tag{3.18}$$

To distinguish the notations of the thickness of film from differentials, we use the roman d for sample thickness. The value n' that enters $k'_x \approx \frac{2\pi n'}{\mathrm{d}}$ can be found from the energy conservation law:

$$\mathbf{k}^2 + k_x^2 = (\mathbf{k} + 2\mathbf{Q})^2 + k_x'^2 \tag{3.19}$$

The first interaction Hamiltonian is always much less than the second one since the derivative of the transverse wave function $d_x \eta_{\mathbf{k},n} = d_x \left(\sqrt{2/\mathrm{d}} \cos k_x x\right) = -k_x \sqrt{2/\mathrm{d}} \sin k_x x$ is proportional to the first power of the large wave vector k_x, whereas the second term contains the square of this large wave vector. Neglecting also the terms $\mathbf{Q}^2 - 4\mathbf{kQ}$ in the first round bracket of eq. (3.18), we find the dominant term in the 4th-order exchange term:

$$H_{ex4} = \frac{\gamma^2 D}{4A} \sum_{\mathbf{k},n} \mathbf{k}^2 \int\limits_{-\frac{d}{2}}^{\frac{d}{2}} dx \left(\eta_{\mathbf{k},n} \eta_{\mathbf{Q}} \eta^*_{\mathbf{k}+2\mathbf{Q},n'} \eta^*_{-\mathbf{Q}} + c.c.\right) \tag{3.20}$$

The transverse wave functions are real. Therefore the integral we need to calculate is:

$$I = 2 \times \left(\frac{2}{d}\right)^2 \int\limits_{-\frac{d}{2}}^{\frac{d}{2}} dx \cos^2 \frac{2\pi x}{d} \cos k_x x \cos k'_x x \tag{3.21}$$

Employing a simple trigonometric identity, we transform this integral into

$$I = \frac{2}{d^2} \int\limits_{-\frac{d}{2}}^{\frac{d}{2}} dx \left(1 + \cos \frac{4\pi x}{d}\right) \left[\cos\left(k_x - k'_x\right) x + \cos\left(k_x + k'_x\right) x\right] \tag{3.22}$$

Since $\cos\left(k_x + k'_x\right) x$ is a very rapidly oscillating function, its contribution to the integral can be neglected. The difference of two wave vectors $k_x - k'_x$ can be approximately calculated employing eq. (3.19) as

$$k_x - k'_x \simeq -\frac{2\left(\mathbf{kQ}\right)}{k_x} \tag{3.23}$$

Thus, the integral (3.22) can be calculated analytically as

$$I = \frac{2k_x}{d^2}\left\{\frac{1}{\mathbf{kQ}} + \frac{\mathbf{kQ}d^2}{2\left[(\mathbf{kQ})^2 d^2 - 4\pi^2 k_x^2\right]}\right\}\sin\frac{\mathbf{kQ}d}{k_x} \tag{3.24}$$

With this the transition matrix element is:

$$T_{\mathbf{k}k_x,\mathbf{Q}\to\mathbf{k}+2\mathbf{Q}k'_x,-\mathbf{Q}} = \frac{\gamma^2 D\mathbf{k}^2}{4A} I \tag{3.25}$$

Let us introduce abbreviated notations for three-dimensional vectors $k = (\mathbf{k}, k_x)$ and $k' = (\mathbf{k}+2\mathbf{Q}, k'_x)$. The differential of transition probability per unit time in the continuum approximation is:

$$\begin{gathered} dw_{k,\mathbf{Q}\to k',-\mathbf{Q}} = \frac{2\pi}{\hbar}\left|T_{k,\mathbf{Q}\to k',-\mathbf{Q}}\right|^2 \delta\left[\gamma M D\left(k_x'^2 - k_x^2 + 2\mathbf{kQ}\right)\right] \\ \times N_k N_{\mathbf{Q}}\left(N_{k'}+1\right)\left(N_{-\mathbf{Q}}+1\right)\frac{V d^3 k'}{(2\pi)^3}, \end{gathered} \tag{3.26}$$

where $V = A\mathrm{d}$ is the volume of the film. To find the complete probability of transition per unit time or equivalently the rate of flip due to exchange interaction, it is necessary to first integrate over possible finite states. The energy conservation allows making integration over k'_x. After that, we get:

$$\begin{gathered} \int \frac{dw_{k,\mathbf{Q}\to k',-\mathbf{Q}}}{dk'_x} dk'_x = \frac{V}{8\pi^2\hbar\gamma M D}\int \frac{d^2k}{k'_x}\times \\ \left|T_{k,\mathbf{Q}\to k',-\mathbf{Q}}\right|^2 N_k N_{\mathbf{Q}}\left(N_{k'}+1\right)\left(N_{-\mathbf{Q}}+1\right) \end{gathered} \tag{3.27}$$

In this result, the summation over the parallel component of the initial moment is already performed. It is necessary to make an additional summation of the differential probability over k_x that, in the continuous approximation, is equivalent to integration $\mathrm{d}\int dk_x/(2\pi)$. We also need to subtract the rate of the inverse process. Thus, the total condensate magnon change rate due to 4th-order exchange interaction (3.20) can be rewritten as

$$\begin{gathered} \frac{1}{\tau_{ex4}} = \frac{V\mathrm{d}}{16\pi^3\hbar\gamma M D}\int \frac{d^3k}{k'_x}\left|T_{k,\mathbf{Q}\to k',-\mathbf{Q}}\right|^2 \times \\ \left[N_k N_{\mathbf{Q}}\left(N_{k'}+1\right)\left(N_{-\mathbf{Q}}+1\right) - \left(N_k+1\right)\left(N_{\mathbf{Q}}+1\right)N_{k'}N_{-\mathbf{Q}}\right]\frac{d^3k}{(2\pi)^3} \end{gathered} \tag{3.28}$$

In this integral, k'_x must be replaced by the value found from eq. (3.23) and $\mathbf{k}' = \mathbf{k} + 2\mathbf{Q}$. Here N_k are the Planck occupation numbers $N_k = \left(\exp \frac{\gamma M D k^2}{T} - 1\right)^{-1}$. The energy conservation implies $N_k = N_{k'}$. The value $N_{\pm\mathbf{Q}}$ are the number of magnons in two condensate components $N_{\pm\mathbf{Q}} = V n_{\pm}$. Employing these properties and eq. (3.25), we find the following expression for the rate of thee flip process:

$$\frac{1}{\tau_{ex4}} = \frac{\gamma^3 \mathrm{d}^2 D \left| n_+ - n_- \right|}{256 \pi^3 \hbar M} \int \frac{d^3 k}{k'_x} \mathbf{k}^4 I^2 N_k \left(N_k + 1 \right) \tag{3.29}$$

4. TWO-TIME MODEL FOR THE RECOVERING OF MAGNON DENSITY AND CURRENT ALONG Z-AXIS

4.1 Simple theory of experiment I: potential well for magnons

A theory that explains the experimental results for potential well employing two fitting parameters was presented in the article [5]. Here we will present a theory that does not use fitting parameters at all but applies a simplifying assumption. We start with the formulation of basic equations.

The density of magnons $n(z,t)$ and z-component of their current $j_z(z,t) = n(z,t)\,v(z,t)$ obey the modified continuity equation for a stationary process:

$$\frac{dj_z}{dz} = \frac{n_0 - n}{\tau} \tag{4.1}$$

Here $j_z = nv_z$ is the z-component of the current; $\mathbf{v} = \frac{\hbar}{m}\nabla\phi$ is the local velocity of the condensate. On the right-hand side, the two terms in the numerator represent the pumping amplitude and attenuation, respectively. The lifetime τ may depend on the density and other parameters. Further, we omit subscript z in the notations of current and velocity. In experiments, the density of condensate magnons was much larger than that of normal magnons with the momentum comparable to Q. The convective current due to the condensate magnons significantly exceeds the diffusive current of the thermal magnons, although the thermal magnon density is approximately 100 times larger than the condensate density. [8]

The amplitude of the magnon potential energy $u(x,z)$ is associated with the z-component of magnetic field $h(x,z)$ from the current-carrying plate as $u = -2\mu_B h$. This value can be estimated from the general expression for potential as a function of two variables:

$$u(x,z) = -2\mu_B h_0 \left[\arctan\frac{z + l/2}{x + x_0} - \arctan\frac{z - l/2}{x + x_0}\right] \tag{4.2}$$

In calculating the magnetic field of the plate, we neglected the thickness of the plate and non-uniformity in the current distribution. To calculate the average energy per magnon, the potential energy (4.2) must be averaged over x from 0 to d with the statistical weight $2\sin^2\frac{\pi x}{d}$. Simplifying this procedure, we get a rougher but reasonable approximation putting $x = d/2$ in eq. (4.2):

$$\overline{u}\,(z) = -2\mu_B h_0 \left[\arctan\frac{z+l/2}{d/2+x_0} - \arctan\frac{z-l/2}{d/2+x_0}\right] \tag{4.3}$$

The averaged energy $\overline{u}\,(z)$ is an even function of z, negative at any z and going to zero as $-\frac{l(2d+x_0)}{z^2}$ for $z \to \pm\infty$. At $z = 0$, it has minimum $\bar{u}_{\min} = -4\mu_B h_0 \arctan\frac{l}{2d+x_0}$. Since $|\bar{u}_{\min}| \gg \hbar^2/ml^2$ for $h_0 \gg 0.1\,Oe$, the potential well has many levels. The number of levels can be estimated as $\mathscr{N} = \frac{l\sqrt{2m|\overline{u}_{\min}|}}{\hbar} \simeq 50$. The level width is $\Gamma = \hbar/\tau$. With the experimental value of the magnon lifetime within the condensate density peak $\tau_1 = 10^{-7}s$, $\Gamma = 10^{-20}erg = \frac{1}{50}\,|u|_{\min}$. Thus, the energy levels overlap. In this situation, the magnons filling the potential well should be considered as classical particles, since the phase coherence is suppressed by the attenuation. They all have parallel magnetic moments $-2\mu_B$ directed opposite to the magnetic field and spontaneous magnetization. The magnons confined in the peak can be roughly treated as particles inside the infinite in y-direction rod of width l and thickness d. The total interaction energy is the sum of interaction energy for each pair. For most interacting magnon pairs, the line connecting this pair of magnons is almost parallel to the y-axis. These magnon pairs contribute to the major part of interaction energy. Therefore, overall, magnons repel each other. The characteristic value of the interaction energy per particle within the peak is $2\mu_B^2 n_{\max}$.

Equation (4.1) implies that $\frac{dj}{dz}$ is negative at the point $z = 0$. As a consequence of parity, $n\,(z)$ is an even function of z, and $j\,(z)$ is an odd function. Therefore, $j\,(0) = 0$. The current j is negative for $z > 0$. It reaches its minimum $j_{\min}$ at a point z_1, where $\frac{dj}{dz}$ turns zero. According to equation (4.1), this is the same point where the magnon density falls to its equilibrium value $n\,(z_1) = n_0$. The value z_1 has the order of magnitude l. From the experimental curve [5], we find

that $z_1 \approx 12\mu m = 1.2l$. The value $|j_{\min}|$ can be estimated as

$$|j_{\min}| \sim \frac{(n_{\max} - n_0)\, l}{\tau_1}, \tag{4.4}$$

where we denoted τ_1 the relaxation time within the peak. At the point z_1, $\frac{dn}{dz}$ has the same order of magnitude as its average in the peak

$$\frac{dn}{dz} \sim -\frac{n_{\max} - n_0}{l}. \tag{4.5}$$

Therefore, the density of condensate continues to decrease. If it could reach the value $n = 0$, then the magnon lifetime would change from τ_1 in the peak to the much longer lifetime τ_0 of an isolated magnon. The latter can be estimated from the Landau-Lifshitz-Gilbert attenuation constant $\alpha \approx 10^{-5}$ for good YIG crystals and the condensate magnons frequency $\omega_{\min} \approx 10^{10} s^{-1}$ at external magnetic field 600 Oe:

$$\tau_0 = (\alpha \omega_{\min})^{-1} \approx 10^{-5} s$$

It is by two decimal orders larger than τ_1. The reason for such a sharp reduction of the lifetime in the peak is the decoherence in the condensate caused by the large dissipative current j. However, the value $n = 0$ is not attainable since the current $j = nv$ would also be zero. It means that the density reaches minimum value $n_{\min}$ at some point $z_2 > z_1$. We will assume that the lifetime τ_0 persists at the minimum density $n_{\min}$. Then in a vicinity of the point z_2 eq. (4.1) becomes

$$\frac{dj}{dz} = \frac{n_0 - n}{\tau_0} \tag{4.6}$$

Employing equation (4.6) in the entire interval (z_1, z_2) and assuming $z_2 - z_1 \sim l$, the change of

the current in this interval is

$$\delta j = j\left(z_2\right) - j\left(z_1\right) \sim \left|j_{\min}\right| \frac{\tau_1}{\tau_0} \ll \left|j_{\min}\right|$$

The lifetime remains close to τ_0 until the density is close to $n_{\min}$ and decreases when n grows. However, as n approaches the value n_0 the lifetime must go to infinity since the uniform equilibrium condensate remains coherent infinitely long time with the presence of steady state pumping. Therefore, it is reasonable to assume that the large average value $\tau_0 \gg \tau_1$ persists everywhere at $z_2 < z < L/2$.

Thus, at point z_2, the current derivative dj/dz is finite and positive. The second derivative of the current at z_2: $\frac{d^2 j}{dz^2} = -\frac{1}{\tau_0}\frac{dn}{dz}$ is equal to zero. But it becomes negative for $z > z_2$ and asymptotically goes to zero for sufficiently large $z \gg l$. Therefore, the positive value $\frac{dj}{dz}$ gradually decreases for $z > z_2$. Let us define the recovery length L_{rec} at which current vanishes and the stationary coherent condensate is restored. Its lower boundary can be found employing eq. (4.6):

$$L_{rec} = \left|j_{\min}\right| / \left.\frac{dj}{dz}\right|_{z=z_2} = \left|j_{\min}\right| \frac{\tau_0}{n_0 - n_{\min}} \tag{4.7}$$

According to eqs. (4.4) and (4.7), an estimate for L_{rec} can be rewritten as

$$L_{rec} \sim l \frac{n_{\max} - n_0}{n_0 - n_{\min}} \frac{\tau_0}{\tau_1} \gg l \tag{4.8}$$

The experimental data are $\frac{n_{\max}}{n_0} = 5$; $\frac{n_{\min}}{n_0} \approx 0.5$, $\tau_0 \approx 10\mu s$; $\tau_1 \approx 100ns$. With these data $L_{rec} \approx 800l = 8000\mu m = 8mm$. But the linear size of the sample is $L = 4mm$. It occurs that $L_{rec} > L/2$. Since the spins cannot propagate beyond the magnet, the current must be equal to zero at both ends of the sample $z = \pm L/2$. The relaxation of the current from zero to some negative value proceeds on the correlation length for the current. At some $z \to L/2 \gg l$ far away from the control line, the coherence length is independent of l. Two linear sizes that may be relevant are the dipolar length ℓ and the thickness of the film d. The total current is equal to

$j = n_+v_+ + n_-v_- + 2\sqrt{n_+n_-}\cos(2Qz + \phi_+ - \phi_-)$, where $v_\pm = \frac{\hbar}{m^*}\frac{\partial\phi_\pm}{\partial z}$. As we argued earlier, the stationary state is rather weakly asymmetric. Therefore, $n_+ \approx n_- = n/2$. The current averaged over period is $j = nv,\ v = \frac{v_+ + v_-}{2}$. Thus, the average current is established on the length of period $\left(\frac{\pi}{2}\right)^{1/4}\sqrt{\ell d} = 1.12\sqrt{\ell d}$. It plays the role of the current relaxation length. In experiment I, it was equal to $4.9\times10^{-4}mm \ll L/2 = 2mm$. The estimate of the current derivative (4.6) with $n = n_{\min}$ persists in the interval $(z_2, L/2)$.

All these relations can be summarized in the inequality:

$$\frac{n_{max}}{n_0} \gtrsim \frac{n_0 - n_{\min}}{n_0}\frac{L}{2l}\frac{\tau_1}{\tau_0} + 1 \tag{4.9}$$

This inequality is the main result of our simplified theory. The right-hand side of this equation can be considered as a rough estimate of the ratio $\frac{n_{max}}{n_0}$. We did not use the second hydrodynamic equation. Eq. (4.9) shows that $\frac{n_{max}}{n_0}$ becomes independent of the amplitude of inhomogeneous field h_0 or the current I through the plate as soon as the number of states in the potential well for magnons $\mathscr{N} = \frac{l\sqrt{2m|\overline{u}(0)|}}{\hbar}$ becomes much more than 1. In other words, $\frac{n_{max}}{n_0}$ reaches saturation for large current I in the plate.

For experimental data $\frac{n_0 - n_{\min}}{n_0} = 0.5$ and $L/l = 400$ it follows that $\frac{\tau_1}{\tau_0}$ must be about 0.02 to get the experimental value $\frac{n_{max}}{n_0} = 5$. The best fit parameters found in the experiment [1] were $\tau_1 = 130ns$ and $\tau_0 = 10\mu s$. However, the measurements of τ_1 show different values at different positions, from the maximum value 180 ns in the peak to the minimum value 120 ns at $z = 10$ nm. The value of $\tau_0 = 10\mu s$ was not measured in experiment I. It was extracted from the best fit for the magnon mobility, assuming that the dispersion $\omega(k)$ can be approximated quadratically near its minimum. In YIG film, the quadratic approximation is valid only in a small range because $\omega(k)$ is strongly asymmetric at both minima, with $k_z < Q$ side much steeper than the other. As support, note that the local maximum of frequency $\gamma\sqrt{H(H + 4\pi M)}$ locates at $k = 0$. It is separated from the minimum by the interval $k_1 = -Q = -\frac{\left(2\pi^3\right)^{1/4}}{\sqrt{\ell d}}$, whereas the same value of frequency to right of minimum locates at $k_2 = \sqrt{\sqrt{1 + \frac{4\pi M}{H}} - 1/\ell} \gg |k_1|$. For $H = 600Oe$ and $4\pi M = 1750Oe$

the ratio $k_2/\left|k_1\right| \approx 10$.

4.2 Simple theory of experiment I: potential barrier for magnons.

Let us consider the case of a potential barrier. It is described by the same equation (4.2) with positive h_0. We again will use the approximation for averaged potential $u\left(z\right) = 2\mu_B h\left(d/2, z\right)$ defined by eq. (4.3). It reaches its maximum $z = 0$ with

$$u_{\max} = 8\mu_B h_0 \arctan \frac{l}{d + 2x_0} \tag{4.10}$$

The value $p_{\max} = \sqrt{2mu_{\max}}$ determines characteristic (imaginary) momentum at the top of the energy barrier. The tunneling probability T is determined by imaginary action $S = p_{\max} l$ as

$$T = \exp\left(-S/\hbar\right) = \exp\left(-\sqrt{2mu_{\max}}l/\hbar\right) \tag{4.11}$$

We assume $T \ll 1$. It implies that the ratio $S/\hbar$ is greater than 1. But it cannot be too large in the experiment, limited by the resolution of the BLS signal at small condensate density. The minimum density is $n\left(0\right) = n_0 T^2$.

As in the attractive case, the relation between the local density $n\left(z\right)$ and z-component of the current j_z is expressed by equation (4.1). Since $n\left(0\right)/n_0 = T \ll 1$, we conclude that

$$\left.\frac{dj}{dz}\right|_{z=0} \approx \frac{n_0}{\tau_0}, \tag{4.12}$$

where τ_0 is the relaxation time at a very low magnon density. The current j is zero at $z = 0$, and according to eq. (4.12), $\frac{dj}{dz}$ is positive here. Suppose j reaches its maximum value $j_{\max}$ at some point $z_1 \sim l$. At this point, the growing density reaches value $n\left(z_1\right) = n_0$ and $\left.\frac{dj_z}{dz}\right|_{z=z_1} = 0$. The value $j_{\max}$ can be estimated in the same way we estimate $\left|j_{\min}\right|$ in the potential well case. Like eq. (4.4), there is $j_{\max} \approx \frac{n_0 l}{\tau_0}$, and $z_1 \sim l$. For $z > z_1$, the derivative $\frac{dj_z}{dz}$ becomes negative. Thus, the density $n\left(z\right)$ grows and becomes higher than n_0. At $z \sim l$, it reaches its maximum and then starts to decrease. Here, the relaxation time τ_1 may be shorter than in the center because the largest

deviation of $n(z)$ from its equilibrium value n_0 is comparable to n_0. For $z \gtrsim l$, the current must be decreasing at a much faster speed $\frac{dj_z}{dz} \sim -\frac{(n-n_0)}{\tau_1}$.

Therefore, unlike the potential well case, the recovery length of j_z here should be much shorter. On a distance of the order of a few l, the equilibrium density n_0 will be established. This picture agrees with the experimental observations [5]. It is obvious that there is no saturation of $n_{\min}/n_0$ for large h_0 or current I.

5. SUMMARY AND CONCLUSIONS

In this work, the main question we want to discuss is: for the Bose-Einstein condensation of magnons (BECM) in YIG film, how to explain the phenomena found in experiments I and II, and what determines the spatial distribution of condensate magnons.

Chapter 2 introduced the two experiments. Experiment I shows the repulsive nature of magnon interaction, while in Experiment II, they managed to split the condensation magnons into four moving clouds. These two experiments are important because both of their results contradict the existing theory on BECM: the quasi-equilibrium theory. We argue that the equilibrium state of the two-component BECM is never reached, and this can be proved by examining the inter-minima relaxation time $\tau_{min-min}$ against the lifetime of condensate magnons τ_m, and $\tau_{min-min}$ should be much longer than τ_m.

In Chapter 3, we first introduced how to calculate $\tau_{min-min}$ using amplitude representation. The two flipping processes considered are the 4-magnon process and the Compton process. The calculation of $\tau_{min-min}$ due to exchange interaction is performed.

In the end, we proposed the two-time model to explain the phenomena the experiments introduced. This model treats magnons as classical particles carrying magnetic moment $-2\mu_B$. With this model, we also explored the spatial distribution of BECM. The model predicts the ratio of two magnon densities: the density in the middle of the potential well and the density of the equilibrium system without a potential well. We can conclude that: the ratio will increase for a deeper well, but will increase much more slowly if the depth exceeds some critical value (this value is quite small). However, for the potential barrier case, such critical value don't exist, and this ratio decreases steadily as the barrier becomes higher.

The key of the two-time model is that we can capture the flow of magnons using two typical lifetimes, τ_0 and τ_1. Although this is just the starting point, it already allows the two-time model to make many correct predictions. As a new model to deal with the spatial distribution of BECM, we expect that more detailed calculations of magnon interaction will help it make more predictions

about this system.

REFERENCES

[1] S. O. Demokritov, V. E. Demidov, O. Dzyapko, G. A. Melkov, A. A. Serga, B. Hillebrands, and A. N. Slavin, "Bose-Einstein condensation of quasi-equilibrium magnons at room temperature under pumping," *Nature*, vol. 443, no. 7110, pp. 430–433, 2006.

[2] E. B. Sonin, "Spin superfluidity and spin waves in YIG films," *Phys. Rev. B*, vol. 95, p. 144432, Apr 2017.

[3] P. Nowik-Boltyk, O. Dzyapko, V. E. Demidov, N. G. Berloff, and S. O. Demokritov, "Spatially non-uniform ground state and quantized vortices in a two-component Bose-Einstein condensate of magnons," *Scientific Reports*, vol. 2, no. 1, p. 482, 2012.

[4] F. Li, W. M. Saslow, and V. L. Pokrovsky, "Phase Diagram for Magnon Condensate in Yttrium Iron Garnet Film," *Scientific Reports*, vol. 3, no. 1, p. 1372, 2013.

[5] I. V. Borisenko, B. Divinskiy, V. E. Demidov, G. Li, T. Nattermann, V. L. Pokrovsky, and S. O. Demokritov, "Direct evidence of spatial stability of Bose-Einstein condensate of magnons," *Nature Communications*, vol. 11, no. 1, p. 1691, 2020.

[6] I. V. Borisenko, V. E. Demidov, V. L. Pokrovsky, and S. O. Demokritov, "Spatial separation of degenerate components of magnon Bose-Einstein condensate by using a local acceleration potential," *Scientific Reports*, vol. 10, no. 1, p. 14881, 2020.

[7] G. Li, C. Sun, T. Nattermann, and V. L. Pokrovsky, "Long-wave magnons in a ferromagnetic film," *Phys. Rev. B*, vol. 98, p. 014436, Jul 2018.

[8] C. Sun, T. Nattermann, and V. L. Pokrovsky, "Bose-Einstein condensation and superfluidity of magnons in yttrium iron garnet films," *Journal of Physics D Applied Physics*, vol. 50, p. 143002, Apr. 2017.

[9] S. M. Rezende, "Theory of coherence in Bose-Einstein condensation phenomena in a microwave-driven interacting magnon gas," *Phys. Rev. B*, vol. 79, p. 174411, May 2009.

[10] I. S. Tupitsyn, P. C. E. Stamp, and A. L. Burin, "Stability of Bose-Einstein Condensates of Hot Magnons in Yttrium Iron Garnet Films," *Phys. Rev. Lett.*, vol. 100, p. 257202, Jun 2008.

[11] P. Nowik-Boltyk, O. Dzyapko, V. E. Demidov, N. G. Berloff, and S. O. Demokritov, "Spatially non-uniform ground state and quantized vortices in a two-component Bose-Einstein condensate of magnons," *Scientific Reports*, vol. 2, no. 1, p. 482, 2012.

[12] T. Holstein and H. Primakoff, "Field Dependence of the Intrinsic Domain Magnetization of a Ferromagnet," *Phys. Rev.*, vol. 58, pp. 1098–1113, Dec 1940.